

# FAULT SURFACE RUPTURE EXPERIMENTS: A COMPARISON OF DRY AND SATURATED SOILS

Jörgen JOHANSSON<sup>1</sup> and Kazuo KONAGAI<sup>2</sup>

<sup>1</sup>Research Associate, Institute of Industrial Science, University of Tokyo,  
Tokyo 153-8505, Japan, jorgen@iis.u-tokyo.ac.jp

<sup>2</sup>Professor, Institute of Industrial Science, University of Tokyo,  
Tokyo 153-8505, Japan, konagai@iis.u-tokyo.ac.jp

The effects on the deformation buildup due to a dip-slip fault when pore water is present in a soil has been studied experimentally. The experiment allows only for round fault which is different from the more common 2-D plane strain experiments and dip-slip faults observed in nature, nevertheless the experiments show how the deformations and loads change substantially when water is present in a soil deposit as often is the case in nature. The experiments will serve as a verification basis for numerical tools that will allow for the numerical simulations of fault induced large soil movements and estimate the possible deformations that structures in and on top of soil deposit will undergo.

**Key Words:** Fault surface rupture experiment, saturated soil, large deformation, localization, shear-band, saturated soil, pore pressure.

## 1. Introduction

The 1999 earthquakes in Taiwan and Turkey have shown how great a risk fault surface ruptures is to human lives, buildings and infrastructure. Even though fault surface rupturing is not a new problem, there are very few building codes in the world containing any type provisions for reducing the risks. This may be due to the infrequent occurrence of fault surface ruptures, the great difficulty in preventing damage to infrastructure and buildings affected by the ruptures and also the difficult task of estimating the related permanent deformations due to many unknown factors such as possible fault location, geometry and motion; and mechanical properties of the soil deposit.

In California, United States; New Zealand; and also in Taiwan, after the 1999 earthquake, so called fault zoning acts have been established. A fault zoning act prevents construction within a certain distance of the known fault line and may be one way of reducing the risks for new buildings and infrastructure, but for structure already built along a fault line other remedial measures are needed, further more the fault zoning act does not say anything about the possible extent of deformations and/or the probability of occurrence of these deformations.

In highly populated countries such as Japan and other east and south-east Asian countries it is difficult to impose a fault-zoning act due to the lack of space. In these countries building code provisions based on engineer-

ing principles are needed as to allow for construction along fault-lines if certain design requirements are met. Such building code provisions would also be attractive for less populated countries, such as United States and New Zealand, as well, since it may allow for more economical construction.

Another issue is the difference between strike-slip and dip-slip faults. The deformations along a strike-slip seem to be concentrated in a narrower zone along the fault line whereas the deformations along a dip-slip fault may affect areas further away from the fault line.<sup>(1)</sup> In Japan there are some 90 dip-slip fault systems with several faults in each system and with a lot of buildings and infrastructure along them.

To provide results in the form of possible extent and probabilities of deformation along these fault lines, much research is needed. Previous research have mostly focused on dry cohesion-less<sup>(2)</sup> or clay materials in 1g-<sup>(3)</sup> and centrifuge tests.<sup>(4)</sup>

The experiments described within here show how the deformations and loads change substantially when water is present in a soil deposit as often is the case in nature. The experiments serves will serve as verification basis for a numerical tool<sup>(5)</sup> that allow for the numerical simulations of fault induced large soil movements and estimate the possible deformations that structures in and on top of soil deposit will undergo.

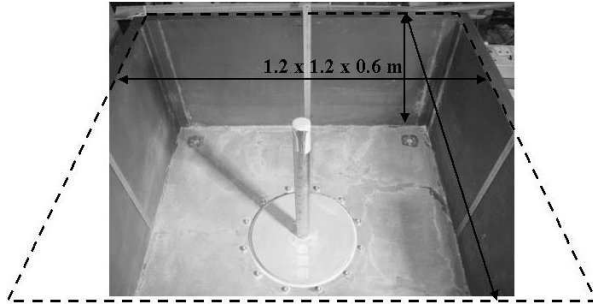


**Figure 1:** View inside the experiment box

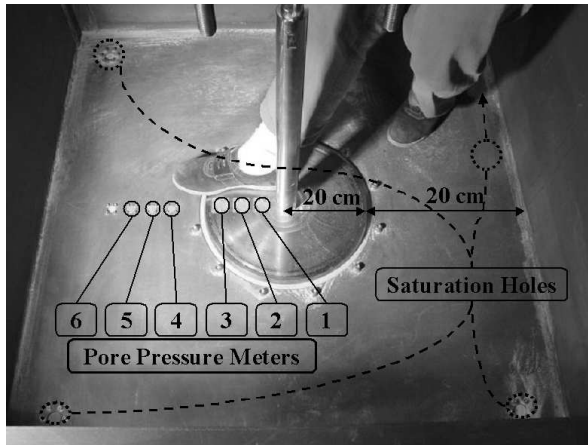


**Figure 2:** Pressure meters and saturation inlets.

## 2. Experiment setup and preparation

To study in detail the effects on the deformation buildup due to a dip-slip fault when pore water is present in a soil a new model experimental box has been designed and constructed as part of larger project involving fault surface ruptures. As can be seen in **Figure 1** the box allows only for axisymmetric fault experiment which is different from the more common 2-D plane strain experiments performed by other researchers. The box was designed with a round piston to simplify the construction of the water-proof box. A prototype structure is not considered rather these experiments will serve as a verification basis for numerical tools in which the experiment could be simulated with an axi-symmetric or 3-D model; or approximately simulated with a 2-D plain strain model. Nevertheless the experiment show many interesting features, which are discussed below.

The box (see **Figure 1**) measures 1.2 by 1.2 meters in plan and is 60 cm deep. The 40 cm diameter piston, attached to a 300 kN hydraulic actuator (see **Figure 3**), was lifted/pushed up through the soil to model a fault offset and induce the subsequent fault surface rupture.

In all experiments the piston displacement (vertical) was given as step function with smooth transition of

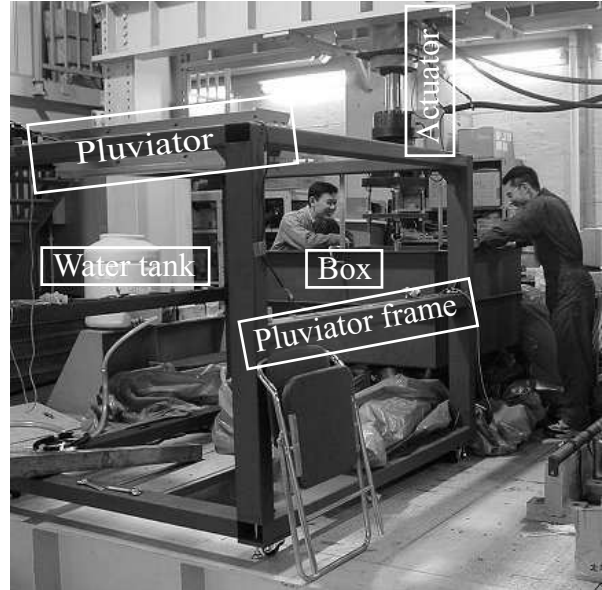


**Figure 3:** Experiment setup.

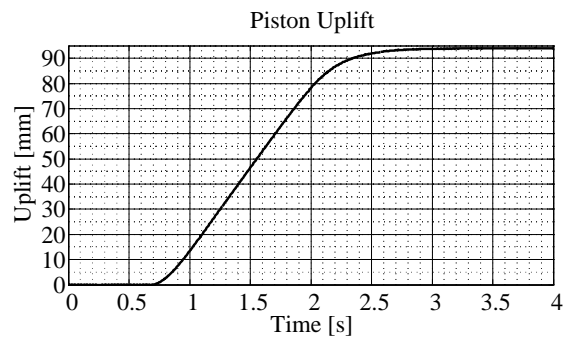


**Figure 4:** Piston Uplift.

from zero to a maximum velocity of 6.5 cm/s and then a smooth transition to zero velocity resulting in a total uplift of 9.4 cm as shown by **Figure 4**.

In the bottom of the box and on top of the piston 6 pore pressure meters were installed (see **Figure 2(b)**).

Toyoura sand with a mean diameter,  $D_{50}$ , of 0.2 mm was air-pluviated into the box to assure repeatability and homogeneity with a pluviator with a wedge-shaped section with a box-wide slit opening of 0.8 mm moving back and fourth along the box at a fixed height. The sand fall height varied between 0.8 and 1.2 meters causing the void ratio to vary between 0.67 and 0.68 from the bottom to the top of the sand. A void ratio of 0.68 gives a density of  $1580 \text{ kg/m}^3$ . To even out the sand thickness differences during the pluviation procedure, scraping was *not* used rather sand was only allowed to exit from the pluviator over areas of lower thickness. To be able to see the induced deformation the sand deposit

**Table 1:** Experiment Parameters.

Material	Toyoura Sand
Mean diameter, $D_{50}$	0.2 mm
Density, $\rho$	1580 kg/m <sup>3</sup>
Void ratio, $e$	0.68
Saturation degree, $S$	80 %
Sand height, $H_{soil}$	40 cm
Piston Uplift, $u_{piston}$	9.4 cm

was inter-layered with thin (3-5 mm) horizontal layers of colored toyoura sand every 5 cm (see **Figure 7**). The total height of the sand was approximately 40 cm.

Three out of the total five experiments were saturated with regular tap water from an elevated water tank with 4 equal long hoses connected close to the corners at the bottom of the box. The saturation time varied between 15 and 20 hours depending on the amount of water in and the elevation of the tank. The elevation was regulated with a small crane at intervals to keep the water inflow approximately constant. An average saturation degree,  $S$ , of 80% was estimated by computing the voids volume and the water volume in the box. (The two dry experiments were saturated after the experiment to allow for sectioning). The experimental parameters are summarized in **Table 1**.

### 3. Experiment results

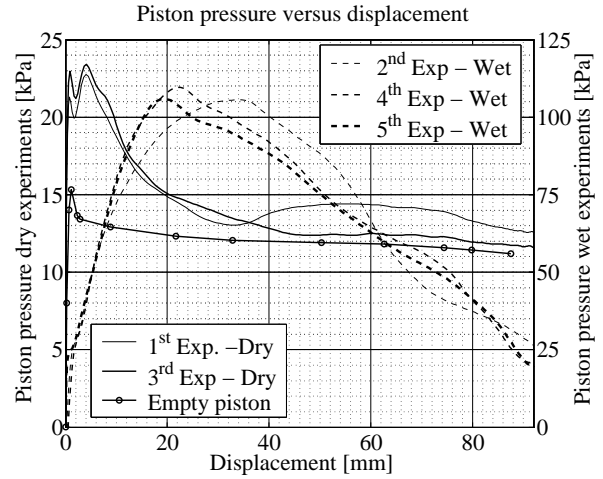
Several different measurements were performed during and after the experiments. They include actuator load and displacement, pore pressures, surface displacements, wave speeds, sand densities water contents etc. Below a few selected data are given and analyzed.

To remove higher frequency noise, a square or cosine window of varying length was convoluted with the raw data. Some of the curves' smoothness differs due to different window length used during the data processing.

#### (1) Piston pressure versus displacement

**Figure 5** shows corrected actuator load normalized with the piston area (0.13 m<sup>2</sup>) plotted versus the piston displacement.

The pressure-displacement curves show an initial sudden peak and drop during the 1st mm displacement and then the pressure increases to reach a second peak at displacements of about 5 mm and 20-30 mm for the dry and wet experiments, respectively. The initial peak is an artifact due to a viscous stick-slip behavior of the actuator piston system, which is primarily caused by the Teflon fitting ring between the piston and the outer fixed cylinder. Several piston uplifts without any sand were performed and the inset in **Figure 5** shows an initial peak of some 35-40 kPa and then piston resistance drops off

**Figure 5:** Piston Pressure versus Displacement.

to a level of about 25 kPa. The self-weight of the piston corresponds to a 8.7 kPa pressure. The crossed curve is an average of all empty piston uplifts (estimated visually). The experimental data was corrected only by subtracting the residual value of 25 kPa from all data points, since it was considered tedious e.g. to correctly subtract the average curve for piston resistance versus displacement since the initial peaks occurs at different points in the actuator load-displacement time histories. The data could be further corrected considering that the piston resistance reduces from about 30 kPa at 1 to 2 mm displacement to about 25 kPa at 15 mm displacement, but was not considered necessary here.

**Figure 5** clearly shows the difference in piston pressure level between a dry and wet experiment and also how the peak piston pressure occurs at a larger displacement for the wet sand. For experiment 5 the second piston pressure peak coincides with the pore pressure peak for a piston uplift of 20 mm.

#### (2) Pore Pressure

**Figure 6** shows the pore pressures for the 6 pressure meters for experiments 3 (inset) and 5. (The pore pressure meters were set to zero before the experiment as to only measure excessive pressures built up during the experiment). In the dry experiment 3 the pore air pressure was measured and a maximum suction of 1.5 kPa was observed at pore pressure meter 1 (pp1). For the wet experiment 5 the maximum negative pore pressure was 28 kPa. For reference the at rest static dry soil pressure is about 6 kPa (compressive).

The pressure peaks occur first at pressure meters closer to the piston edge, i.e. closer to the rupture zone and then at the pressure meters away from the rupture, either toward the middle of the piston or towards side of the box, for both dry and wet cases. The radial configuration of the experiment should cause magnification

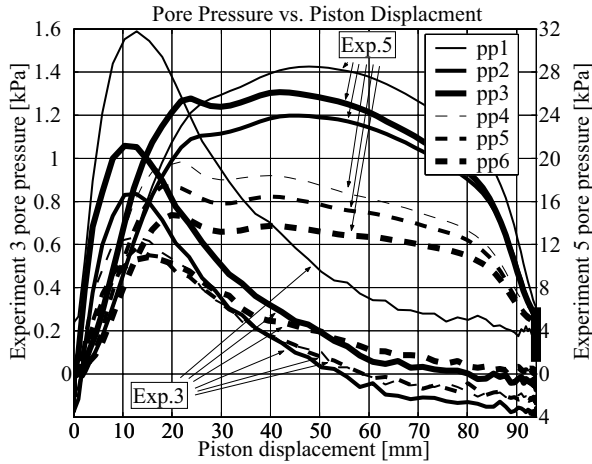


**Figure 6:** Pore pressure versus piston displacement for exp. 3 and 5.

of the pressures closer to the piston center and this is confirmed by the higher negative pressures measured at pp1.

The curves for pore pressure meters 1-6 for the wet experiment 5 there are two peaks, one at around 20 mm and one at between 40-45 mm displacement, which seem to correlate with the offsets in the white solid line in the section **Figure 7(b)**. The solid line is smoothly bent upward some 20 mm until it reaches a localization band and then it reaches a second localization band with a total offset of some 50 mm vertical from the originally horizontal line (dashed line in the figure).

### (3) Sections and Surface shapes

After the experiments the box was drained and the moist sand could be sectioned to study the deformations built up in the sand. For each experiment several sections were carefully cut, brushed and water-sprayed to obtain a smooth surfaces for taking photos; Two section from the dry experiment 3 and the wet experiment 5 are shown in **Figure 7**. The soil deformation has localized into several about 2 to 3 mm wide bands and offset the dark horizontal lines. The shear-band or localization bands are readily seen as brighter lines crossing through darker less deformed zones. (When spraying water on the section before taking the photos, the localized bands, having a higher void ratio due to dilation during the experiments, dries out faster and leave dry bright lines in the darker moist surrounding soil.)

The sequence of the localization is from right to left i.e. the shear-band farthest away from the piston occurs first and the mainly vertical shear-band occurs last as others also report.<sup>(6,4)</sup>

In the saturated case soil further away from the localization band is deformed, indicating that a larger part of the soil deformed before the deformation localization

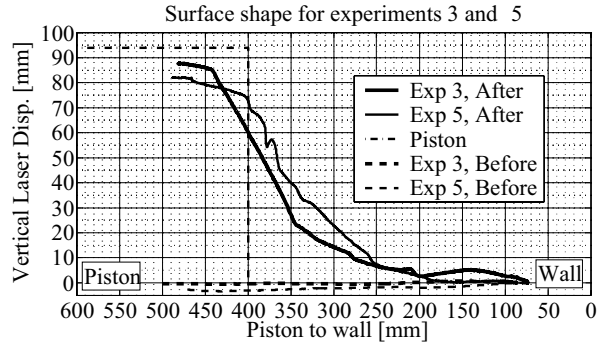


**Figure 8:** Surface shapes for experiment 3 and 5.

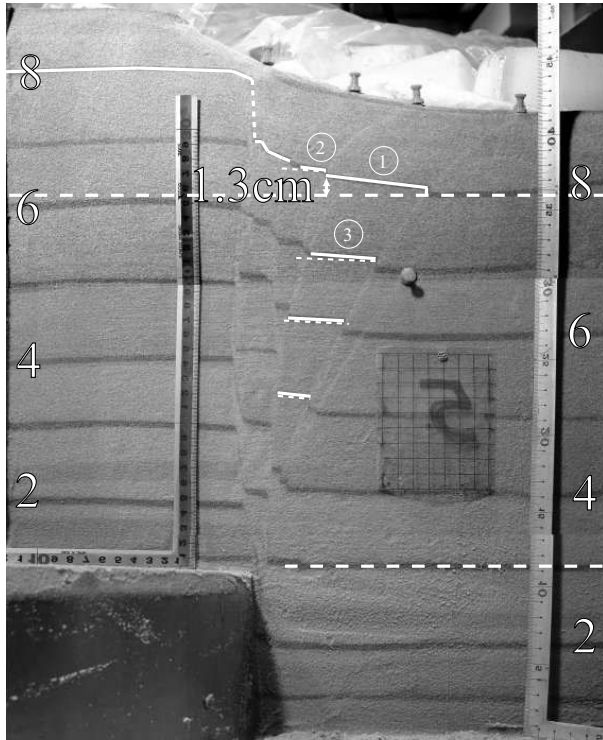
occurred. The horizontal white dashed lines are added as guides to the eye to see the upward bending of the soil when approaching the rupture. The negative pore water pressure increases the effective stresses, thus increasing the failure strength of the soil, which then behaves elastically during a larger deformation than in the dry sand experiments, which is confirmed by the much higher pressure in the pressure displacement graph (see **Figure 5**) for the wet experiments. The inclinations of the numbered lines in **Figure 7** are given in **Table 2**. The inclination is generally larger for the wet experiment 5.

**Surface shape:** **Figure 8** shows the surface shape before and after the experiments, which were measured with laser range meters. The piston center is located at 600 mm in the left part of figure and the box wall is in the right part at 0 mm. As can be seen the curves only reach partially into area over the piston center because the actuator connection was in the way for the laser range meter. The curves did reach a plateau and the sand surface, which could not be measured, is approximately horizontal all around the piston center.

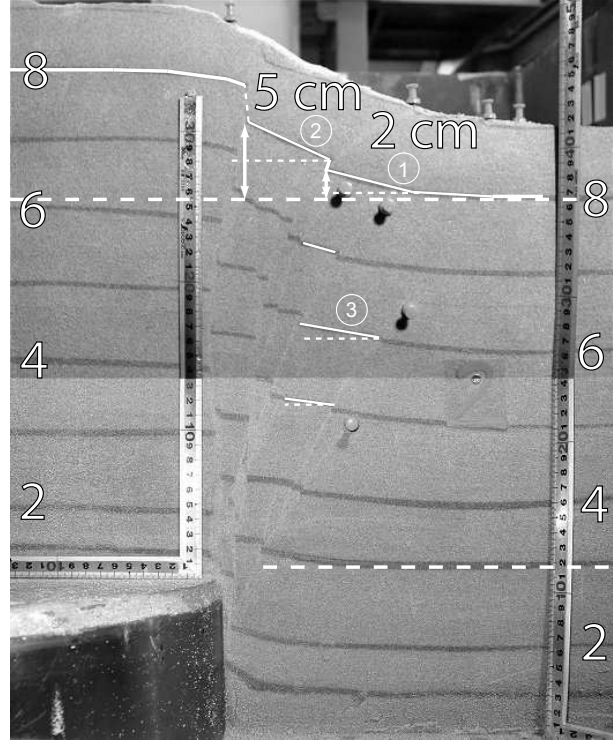
**Compression:** Both the laser surface shape measurements and measurements from the section photos indicate that the uplift of the surface above the piston is less than the piston uplift i.e. some vertical compression (see **Table 2**) occurred during the experiment. The compression was computed as:

$$\varepsilon = \frac{u_{\text{surface}} - u_{\text{piston}}}{H_{\text{soil}}}$$

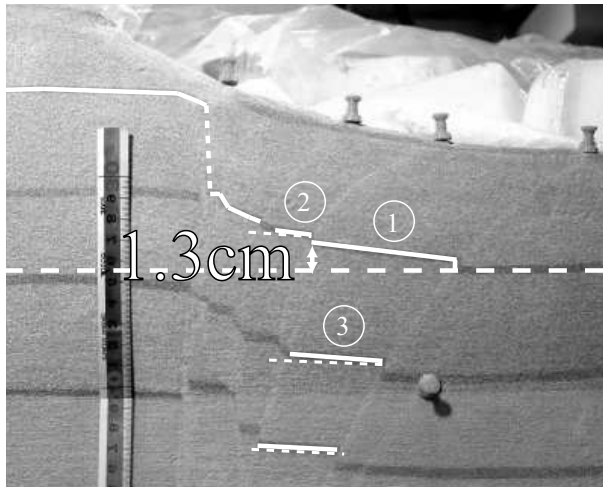
Where,  $u_{\text{surface}}$  and  $u_{\text{piston}}$  are the surface and piston uplift respectively.  $H_{\text{soil}}$  is the original soil deposit thickness. The section photos gives a larger compression than the ones computed from the laser surface measurements. There may be several reasons for the difference. Firstly the photos may be distorted and the obtained measurements would therefore be incorrect even though the measurements were carefully scaled with the rulers



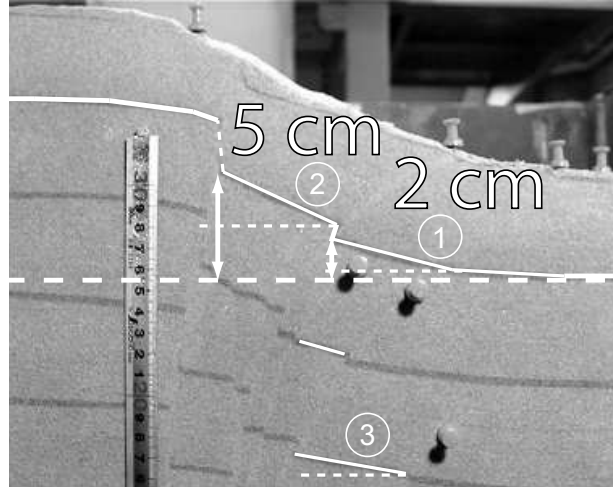
(a) Experiment 3 - dry



(b) Experiment 5 - wet



(c) Exp. 3 enlargement of upper part.



(d) Exp. 5 enlargement of upper part.

**Figure 7:** Section cut from dry and wet experiment.

present in the photos. Secondly the photos were taken after the soil was drained. During the drainage procedure after the experiment the effective stresses increased and some extra compression may have occurred.

#### 4. Conclusions

Important observations from the dry and wet fault surface rupture experiments are:

- The required actuator load (piston pressure) to cause the rupture is substantially (almost 5 times) larger

for the wet soil.

- The deformations seem to localize at a later stage for the wet soil indicated by the piston pressure displacement curve and also observed in the sections where the initially horizontal lines are more inclined for the wet soil.
- The peaks in piston pressure and pore pressure are strongly correlated.
- The surface shape measurements indicate that the

**Table 2:** Compression of soil on top of piston.

Experiment	3	5
Total uplift at surface, laser [mm]	88	85
Compression of sand deposit, laser [%]	1.5	2.3
Compression of sand deposit, photo [%]	4.3	4.2
Inclination of line 1 [%]	12	26
Inclination of line 2 [%]	12	46
Inclination of line 3 [%]	7.6	17

soil above the piston was compressed a similar amount for the dry and wet soil.

**ACKNOWLEDGMENT:** We would like to thank everyone who helped the first author while preparing for and performing the experiments. This research was supported by a part of the grant-in-aid No. 12355020 for scientific research (A) from the Japan Society for the Promotion of Science and is gratefully acknowledged. The first author also acknowledges the financial support in form a doctoral study scholarship by the Ministry of Education, Sports, and Culture of Japan.

#### REFERENCES

- 1) Mukoyama, S.: Fault induced surface configuration features (in japanese), *Mountain Geomorphology*, 82–100, Kokonshoin Press, 2000.
- 2) Cole, D. A. J. and Lade, P. V.: Influence zones in alluvium over dip-slip faults, *Journal of Geotechnical Engineering*, **110**(5), 597–615, 1984.
- 3) Bray, J. D., Seed, R. B., Cluff, L. S. and Seed, H. B.: Earthquake fault rupture propagation through soil, *Journal of Geotechnical Engineering*, **120**(3), 543–580, 1990.
- 4) Stone, K. J. L. and Wood, D.: Effects of dilatancy and particle size observed in model tests on sand, *Soils and Foundations*, **32**(4), 43–57, 1992.
- 5) Johansson, J. and Konagai, K.: Modeling of large deformations of saturated soils during fault surface ruptures., *Bulletin of earthquake resistant structure research center*, 36, 17–34, Earthquake resistant structure research center, Institute of Industrial Science, University of Tokyo, 2003.
- 6) Lade, P. V. and Cole, D. A. J.: Multiple failure surfaces over dip-slip faults, *Journal of Geotechnical Engineering*, **110**(5), 616–627, 1984.

(Received July 10, 2003)